**H1-prelim-02-076**
April 2002

# Measurement of Inclusive $D$-meson Production in Deep Inelastic Scattering at HERA

H1 Collaboration

**Abstract**

The inclusive production of charmed mesons in deep inelastic scattering is studied with the H1 detector at HERA. Inclusive production cross sections are measured for the vector- $D^*$ and for the pseudoscalar charmed mesons $D^0, D_S$ and, for the first time at HERA, also $D^+$ mesons. The finite lifetimes of 0.4 to 1 ps for the pseudoscalar mesons lead to a separation of their production and decay vertices, which is exploited to distinguish signal and background processes and to substantially improve the signal qualities. Differential distributions are measured for the $D^+$ and $D^0$ mesons and compared with predictions, based on LO Monte Carlo simulations.

The measured production cross sections are used to test the isospin invariance of the fragmentation process and to extract the strangeness suppression factor $\gamma_s$ and the fraction $P_V$ of D-mesons produced in a vector state. The results are compared with values measured e.g. at $e^+e^-$-colliders and allow tests of the assumed universality of the charm fragmentation process.

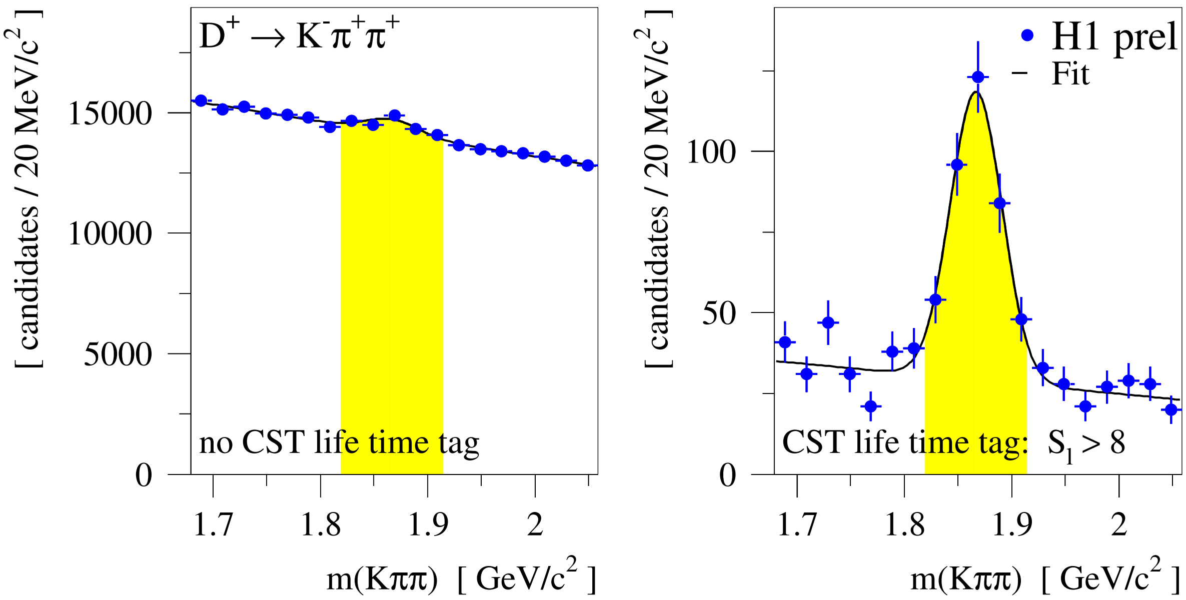


Figure 1: Comparison of the invariant mass distributions $m(K\pi\pi)$ for $D^+ \to K^-\pi^+\pi^+$ decay candidates (a) before and (b) after a cut on the decay length significance $S_l = l/\sigma_l > 8$, where $l$ is the radial separation distance between the meson production and its decay vertex, and $\sigma_l$ the error of $l$. The background contribution is suppressed by $\mathcal{O}(300)$ and the signal to background ratio is improved by a factor $\mathcal{O}(50)$ when vertexing information measured with the H1 central Si vertex detector CST is exploited.

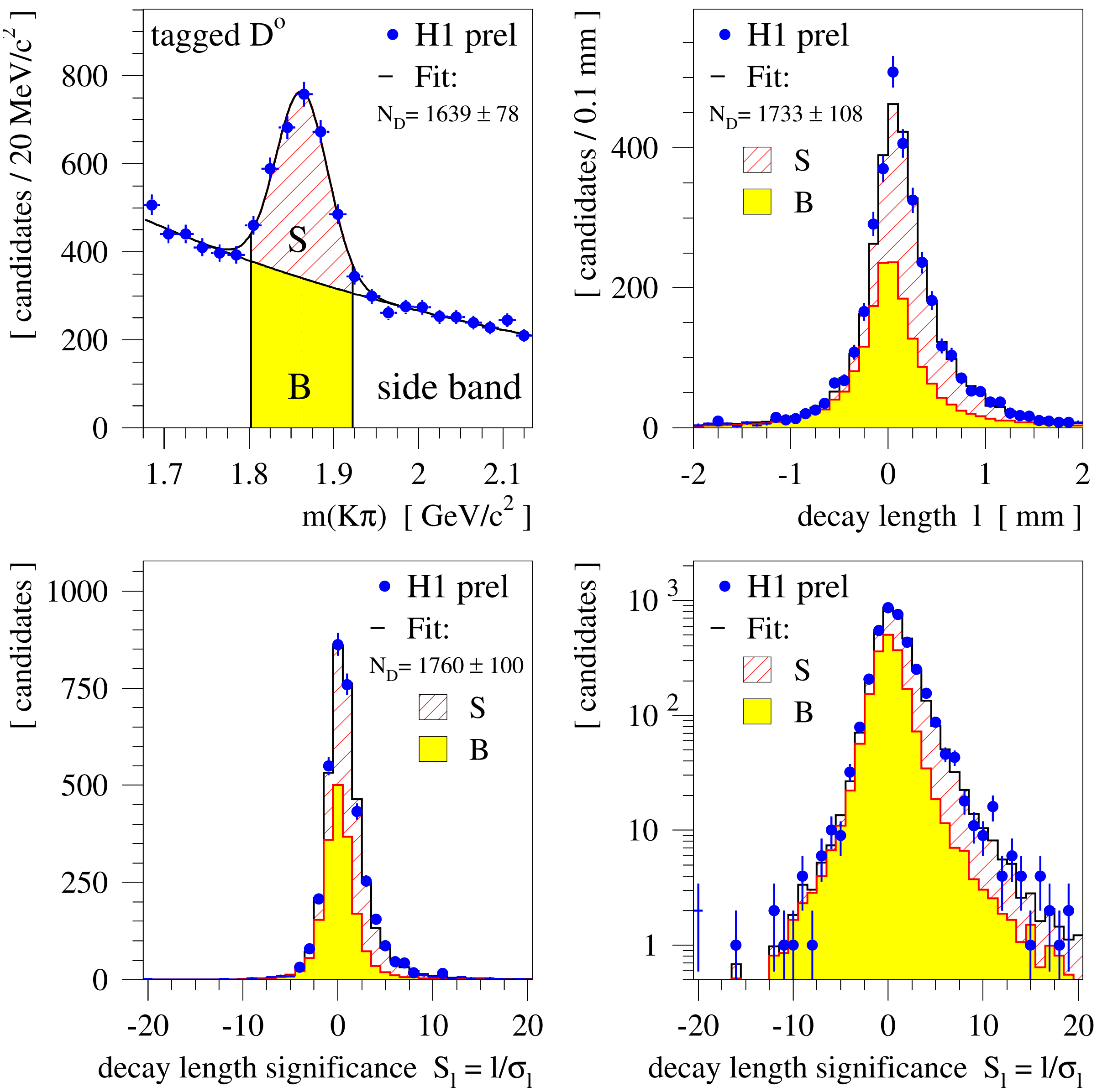


Figure 2: a) $K\pi$-invariant mass distribution for tagged $D^0 \rightarrow K^-\pi^+$ decay candidates (*tagged* denotes the cases where the $D^0$ is explicitly known to originate from a $D^*$ decay); b) the decay length distribution composed of the background contribution (yellow) taken from the sideband in the data (which represents directly the achieved resolution function), and the signal contribution, the shape of which is taken from the simulation. c,d) decay length significance $S_l$ distributions (linear and logarithmic scale); in the fit only the normalisations of signal and background areas are determined; the independent extraction methods produce compatible numbers of signal events.

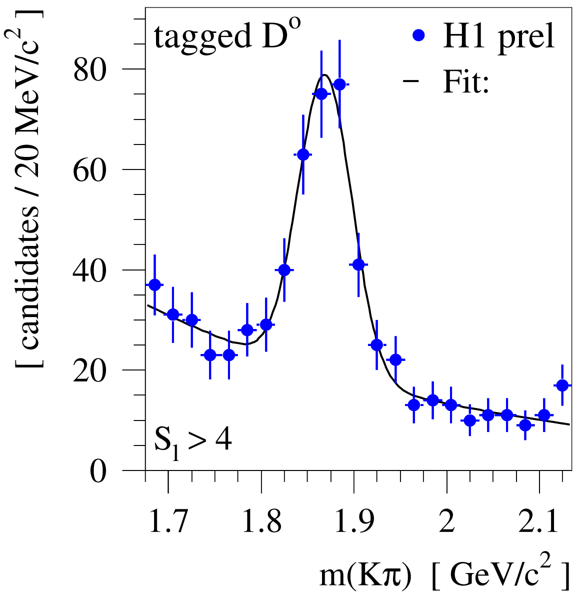


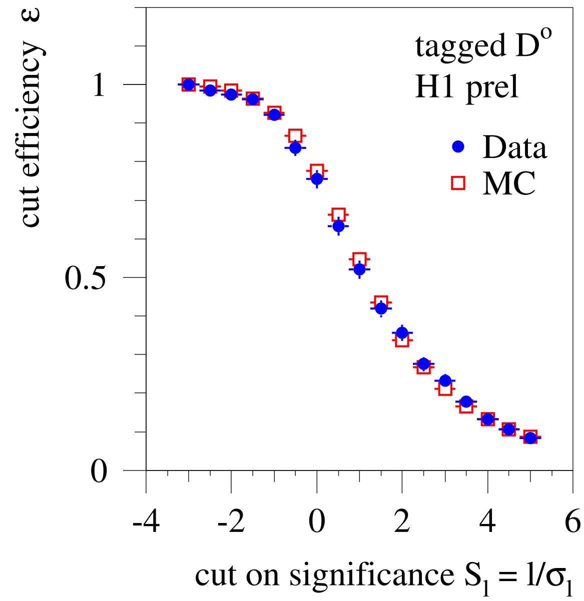


Figure 3: a) $K\pi$-invariant mass distribution for tagged $D^0 \to K^-\pi^+$ decay candidates for a decay length significance $S_l > 4$; b) efficiency distribution as a function of the cut on the decay length significance $S_l = l/\sigma_l$; the efficiency is defined as the number of fitted $D^0$-mesons after applying the cut on $S_l$ divided by the total number of $D^0$-mesons without $S_l$ -cuts. Data (solid dots) are compared with expectations from the simulation (open squares).

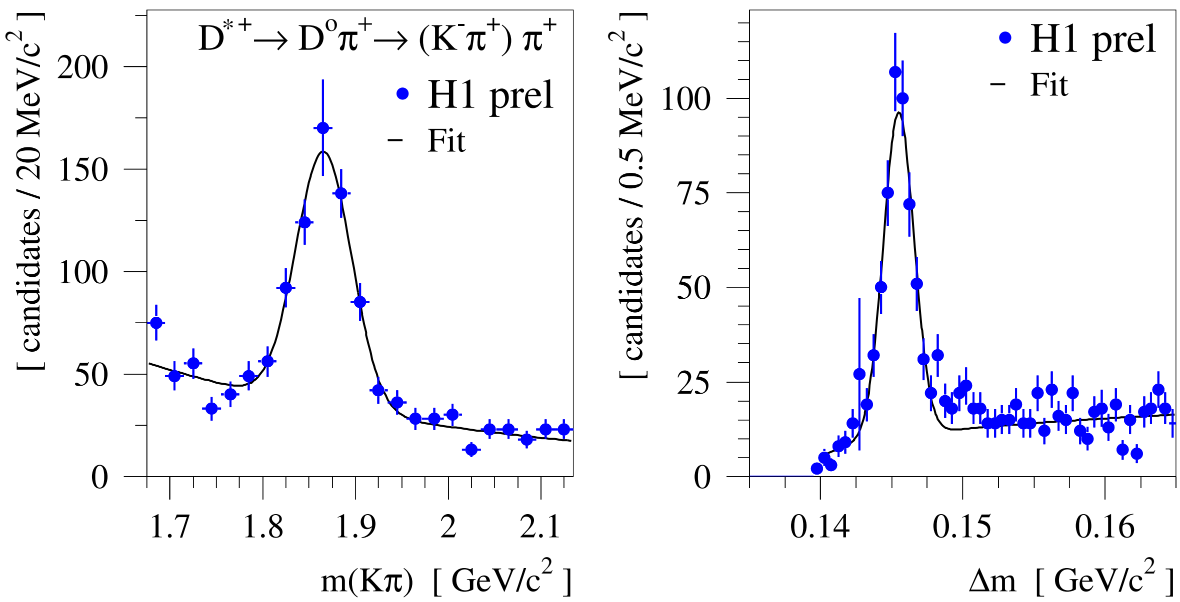


Figure 4: $D^{*+} \to D^0\pi^+ \to (K^-\pi^+)\pi^+$ decay candidate distributions: a) $K\pi$-invariant mass distribution after a $3-\sigma$-cut in the $\Delta M = m(K^-\pi^+)\pi^+) - m(K^-\pi^+)$ - variable, shown in b). The total number of $D^*$ is determined from a fit to the $m(K\pi)$ distribution, as indicated in a).

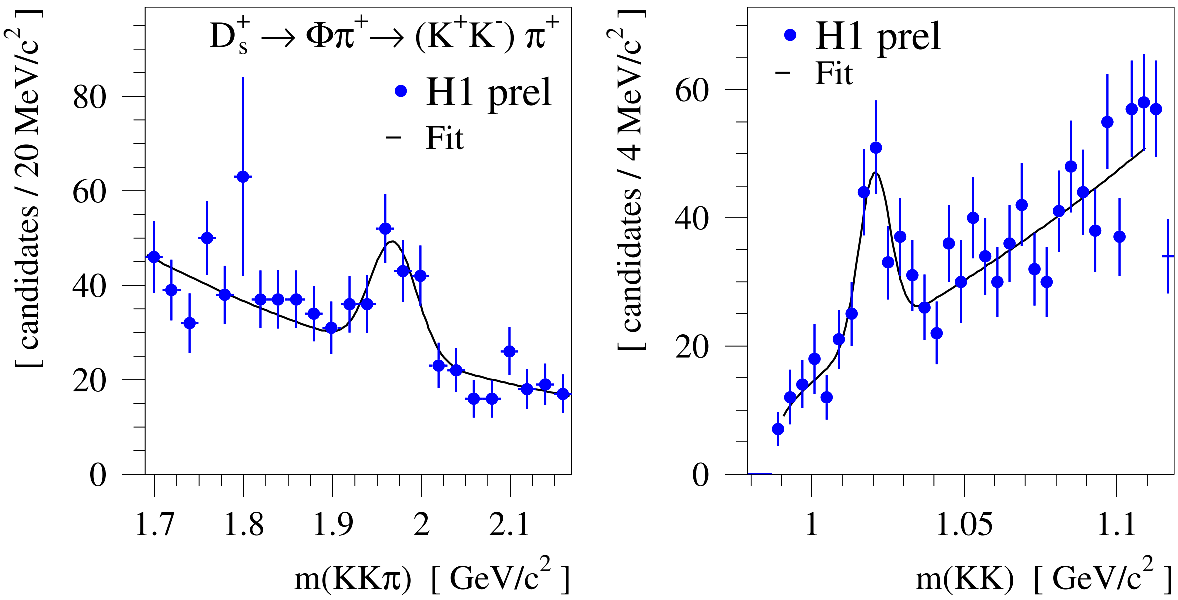


Figure 5: $D_s^+ \to \Phi\pi^+ \to (K^+K^-)\pi^+$ decay candidate distributions: a) invariant mass distribution $m(KK\pi)$ after restricting the $m(KK)$-invariant mass to the $\Phi$-resonance region as shown in b).

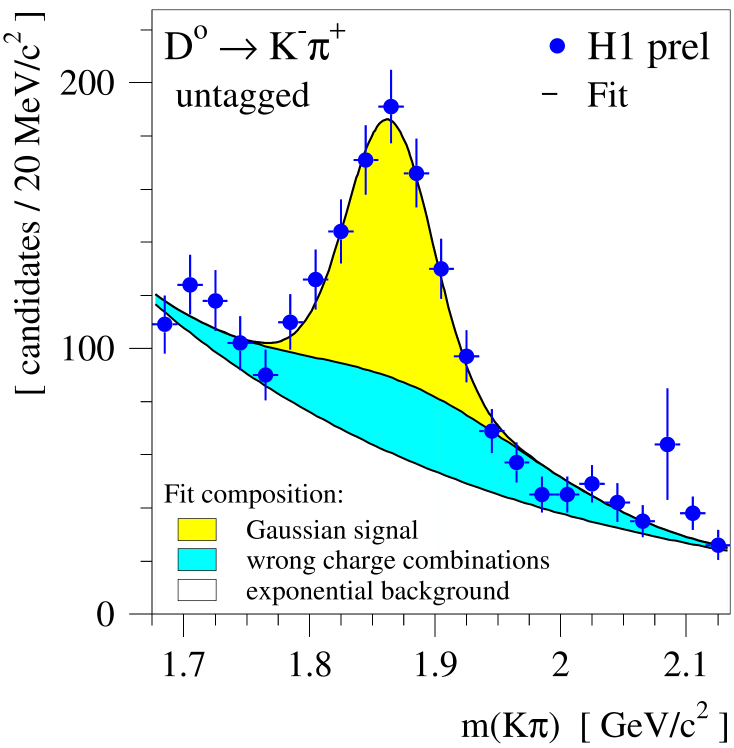


Figure 6: $D^0 \to K^- \pi^+$ decay candidate distribution: the decomposition of the data into a Gaussian right sign signal (bright shading), the wrong sign charge combination (dark shading, function taken from simulation) and an exponential background is separately indicated.

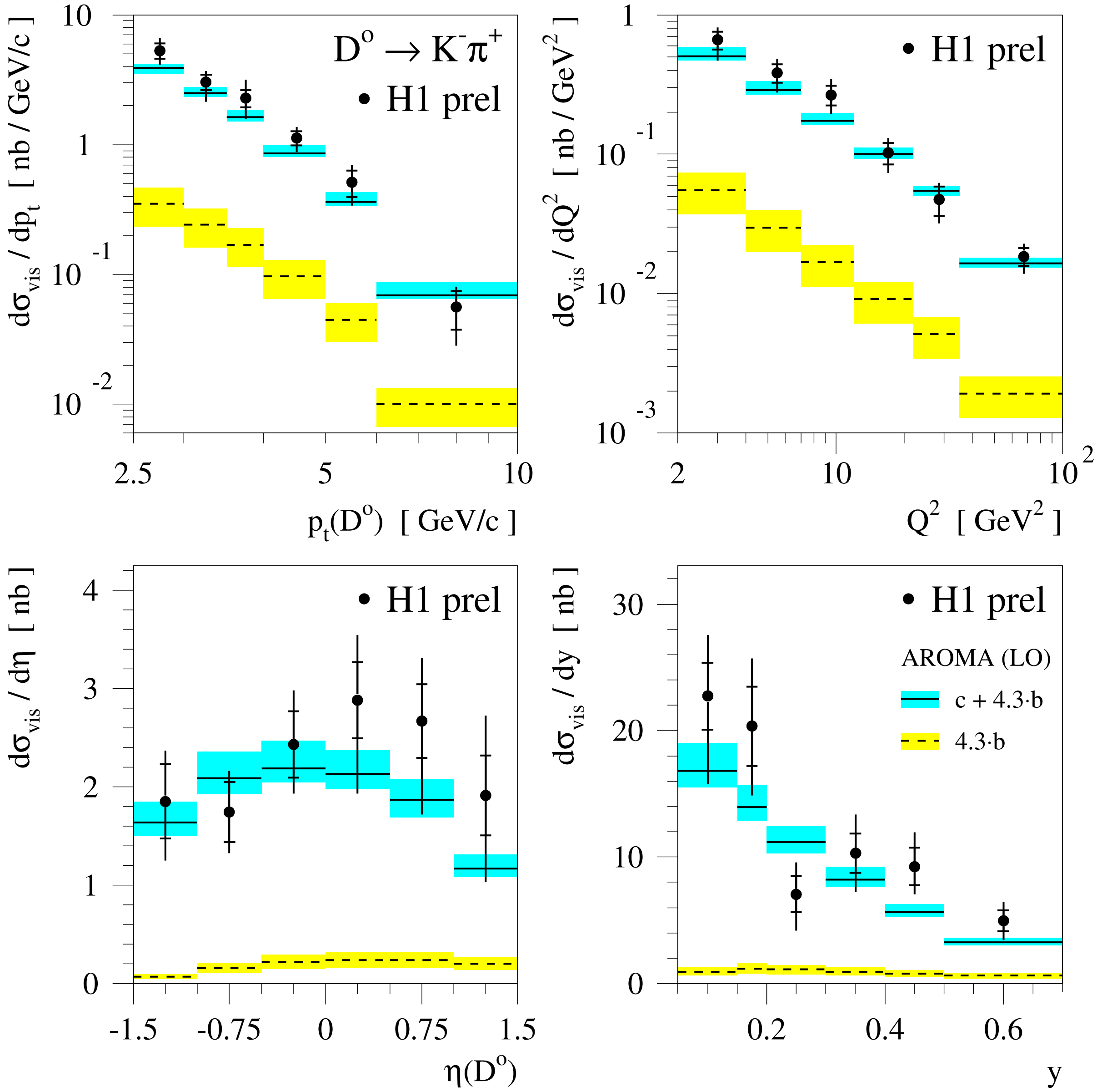


Figure 7: Differential production cross section for untagged $D^0$ mesons as a function of the $D^0$ transverse momentum and pseudorapidity (left) and the event kinematics (right). The dark shaded bands indicate the AROMA Monte Carlo predictions including a scaled beauty contribution, shown separately as light shaded bands. In the simulation the following parameters for the calculations are used: proton structure function: GRV 98 (LO), $m_c = 1.5$ GeV, $m_b = 4.75$ GeV, Peterson parameter $\epsilon_c = 0.078, \epsilon_b = 0.0069$; beauty cross section scale factor $= 4.3 \pm 1.4$, as previously published by H1.

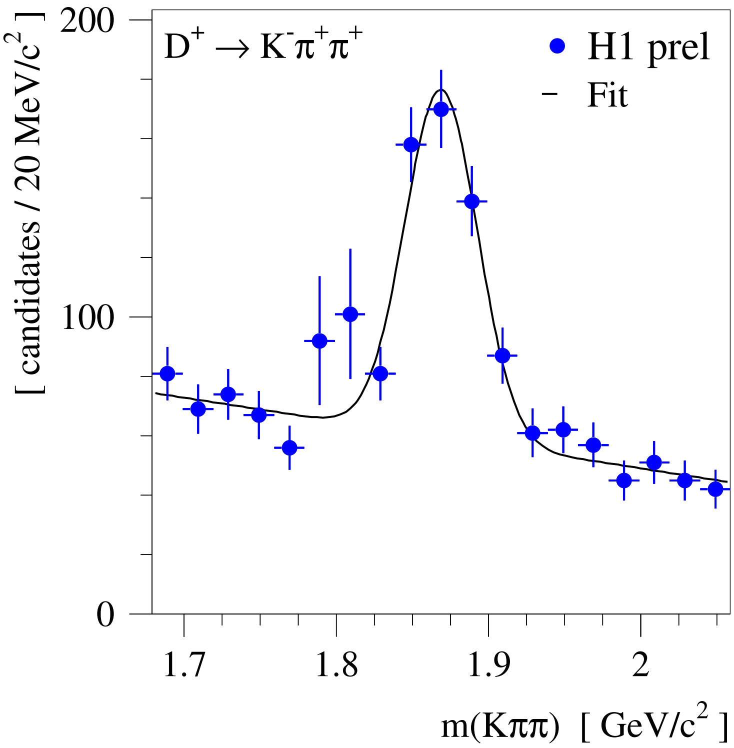


Figure 8: Invariant mass $m(K\pi\pi)$ distribution for $D^+ \rightarrow K^-\pi^+\pi^+$ decay candidates: the curve indicates the fit to the H1 data using a Gaussian function for the signal and a linear for the background (solid dots).

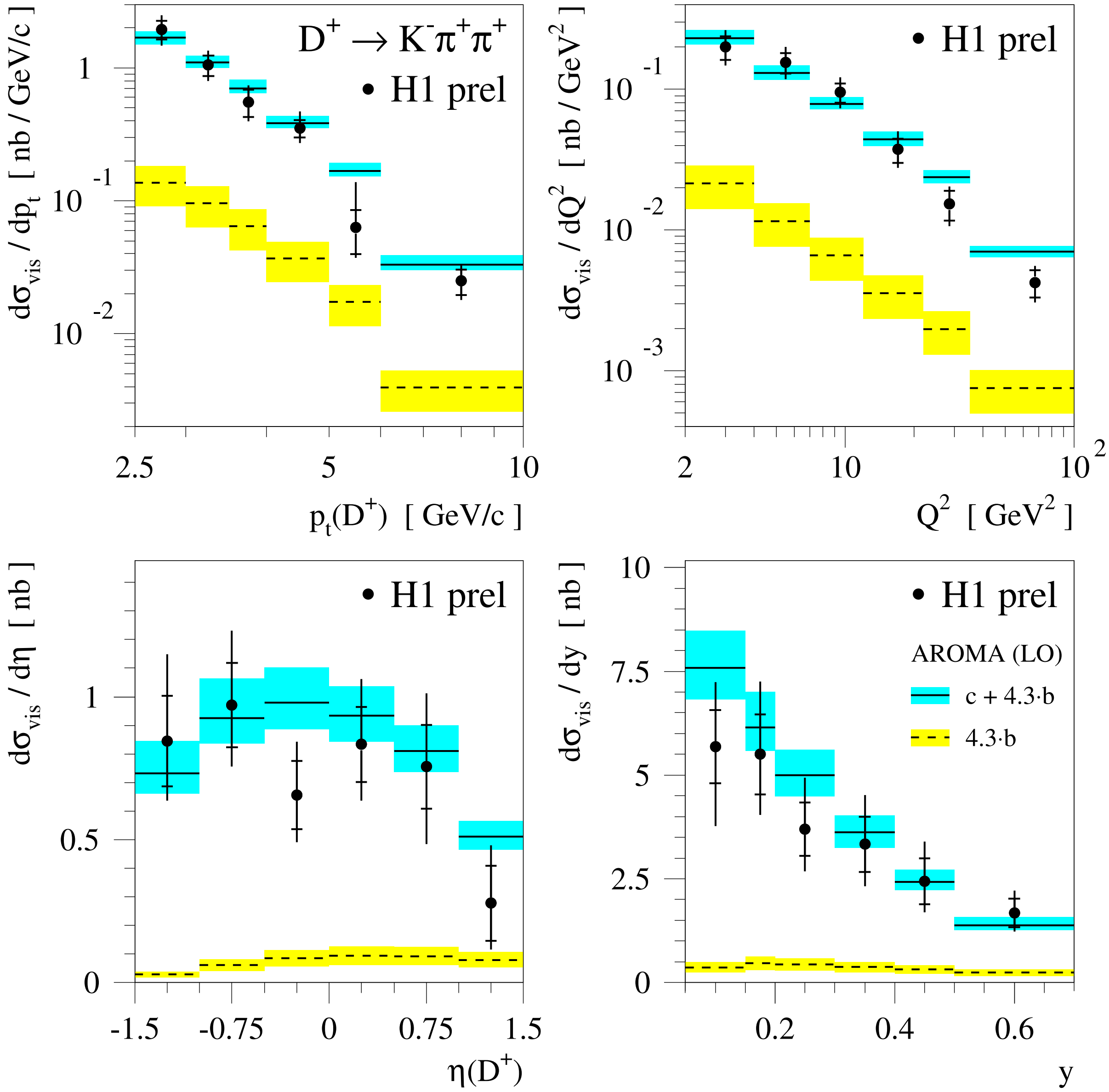


Figure 9: Differential production cross section for $D^+$ as a function of $D^+$ transverse momentum and pseudorapidity (left) event kinematic variables (right). The dark shaded bands indicate the AROMA MC predictions including a scaled beauty contribution, shown separately as light shaded bands. The MC parameters are given in the caption of fig.7.

| **Cross section** | $D^+$ | $D^0$ | $D_s^+$ | $D^{*+}$ |
|---|---|---|---|---|
| $\sigma_{vis}(ep \to eDX)$ (nb) | 2.16 | 6.53 | 1.67 | 2.90 |
| stat. error on $\sigma_{vis}$ | $\pm0.19$ | $\pm0.49$ | $\pm0.41$ | $\pm0.20$ |
| syst. error on $\sigma_{vis}$ | $^{+0.46}_{-0.35}$ | $^{+1.06}_{-1.30}$ | $^{+0.54}_{-0.54}$ | $^{+0.58}_{-0.44}$ |
| AROMA LO prediction $\sigma_{vis}$ | 2.45 | 5.54 | 1.15 | 2.61 |
| error on prediction | $\pm0.30$ | $\pm0.69$ | $\pm0.30$ | $\pm0.31$ |

Table 1: Inclusive charmed meson electroproduction cross sections for the four meson states in the visible kinematic range, defined by $2 \le Q^2 \le 100\,\mathrm{GeV}^2$, $0.05 \le y \le 0.7$, $p_t(D) \ge 2.5\,\mathrm{GeV}/c$ and $|\eta(D)| \le 1.5$.

## Fragmentation Ratios

In order to determine fragmentation ratios, the fragmentation factors $f(c \to D)$ are calculated based on the measured cross sections $\sigma_{vis}$ and the predictions by the AROMA leading order Monte Carlo simulation for both charm $\sigma_{c\bar{c}}^{MC}$ and beauty $\sigma_{b\bar{b}}^{MC}$ as given below:

$$f(c \to D) = \frac{\sigma_{vis} - 2 \cdot \sigma_{b\bar{b}}^{MC} \cdot f(b \to D)}{2 \cdot \sigma_{c\bar{c}}^{MC}} = \frac{\sigma_{vis}(ep \to eDX) - \sigma_{vis}^{MC}(ep \to b\bar{b} \to eDX)}{\frac{\sigma_{vis}^{MC}(ep \to c\bar{c} \to eDX)}{f_{w.a.}(c \to D)}}$$

where $f_{w.a.}$ denotes the current world average value of the relevant fragmentation factor.

| **Fragmentation Factors and Ratios** | $D^+$ | $D^0$ | $D_s^+$ | $D^{*+}$ |
|---|---|---|---|---|
| $f(c \to D)$ | 0.202 | 0.658 | 0.156 | 0.263 |
| stat. error | $\pm 0.020$ | $\pm 0.054$ | $\pm 0.043$ | $\pm 0.019$ |
| syst. error | $^{+0.045}_{-0.033}$ | $^{+0.115}_{-0.148}$ | $^{+0.036}_{-0.035}$ | $^{+0.056}_{-0.042}$ |
| theo. error | $^{+0.029}_{-0.021}$ | $^{+0.086}_{-0.048}$ | $^{+0.050}_{-0.046}$ | $^{+0.031}_{-0.022}$ |
| $f_{w.a.}$ = world average | $0.232 \pm 0.018$ | $0.549 \pm 0.026$ | $0.101 \pm 0.027$ | $0.235 \pm 0.010$ |

Table 2: Fragmentation factors deduced from the measured cross sections. The small b-contributions are subtracted. The obtained values compare well with present world average numbers.

The fragmentation ratios $R_{u/d}$, $\gamma_s$, $P_V$ and $P'_V$ are calculated based on the measured cross sections and the well known decay branching ratios $BR$. Using for convenience the previously introduced fragmentation fractions $f(c \to D)$, the expressions $R_{u/d}$, $\gamma_s$, $P_V$ and $P'_V$ are determined by the expressions listed below. The value $P'_V$ is extracted under the isosopin invariance assumption, i.e. $f(c \to D^{*+}) = f(c \to D^{*0})$.

$$
\begin{aligned}
R_{u/d} &= \frac{f(c \to D^0) - f(c \to D^{*+})\ BR(D^{*+} \to D^0\pi^+)}{f(c \to D^+) + f(c \to D^{*+})\ BR(D^{*+} \to D^0\pi^+)} \\
&= 1.26\ \pm 0.20\ (stat)\ \pm 0.13\ (syst) \pm 0.04\ (theory) \\
&(= 1.00\ \pm 0.09 \qquad \text{world average})
\end{aligned}
$$

$$
\begin{aligned}
\gamma_s &= \frac{2\ f(c \to D_s^+)}{f(c \to D^+) + f(c \to D^o)} \\
&= 0.36 \pm 0.10\ (stat)\ \pm 0.01\ (syst)\ \pm 0.08\ (theory) \\
&(= 0.26\ \pm 0.07 \qquad \text{world average})
\end{aligned}
$$

$$
\begin{aligned}
P_V &= \frac{VM}{PS + VM} \\
&= \frac{f(c \to D^{*+})}{f(c \to D^+) + f(c \to D^{*+})\ BR(D^{*+} \to D^0\pi^+)} \\
&= 0.693\ \pm 0.045\ (stat)\ \pm 0.004\ (syst) \pm 0.009\ (theory) \\
&(= 0.601\ \pm 0.032 \qquad \text{world average})
\end{aligned}
$$

$$
\begin{aligned}
P'_V &= \frac{2\ f(c \to D^{*+})}{f(c \to D^+) + f(c \to D^o)} \\
&= 0.613\ \pm 0.061\ (stat)\ \pm 0.033\ (syst) \pm 0.008\ (theory)
\end{aligned}
$$

## Summary

Production cross sections are measured for the vector- $D^*$ and for the pseudoscalar charmed mesons $D^0$, $D_S$ and, for the first time at HERA, also $D^+$ mesons through their decay $D^+ \to K^-\pi^+\pi^+$. The measurements rely on the proper reconstruction of the vertex separation distance and its error for the $D$-meson decays.

The inclusive $D^*$ production cross sections are within errors in agreement with both previous measurements, and with Monte Carlo predictions, based on the leading order AROMA generator program including parton shower modelling.

Differential cross sections are measured for $D^0$ and $D^+$ mesons as functions of the meson transverse momenta and pseudorapidity, and as functions of the event kinematic variables $y$ and $Q^2$. The measured cross sections are found to be reasonably well described by the LO Monte Carlo predictions.

Based on the measured cross sections, the fragmentation sensitive parameters $P_V$, $R_{u/d}$ and $\gamma_s$ are extracted. They compare well with the present world average values, and as such support the hypothesis of universality of charm fragmentation.